FOCAL MECHANISM DETERMINATION USING WAVEFORM DATA FROM A BROADBAND STATION IN THE PHILIPPINES

Vilma Castillejos Hernandez[*] **Supervisor: Tatsuhiko Hara**[**]
MEE10508

ABSTRACT

We performed time domain moment tensor inversion using broadband waveform data recorded at a broadband seismic station in the Philippines to investigate its applicability. We used a time domain moment tensor inversion code (TDMT_INVc) in this study. The Green's functions are computed by frequency wavenumber integration program. We utilized broadband waveform data recorded at a seismic station at Davao; the station code is DAV. The waveform data were retrieved from the Incorporated Research Institutions for Seismology-Data Management Center (IRIS-DMC). We analyzed two earthquakes that occurred near station DAV. They are the events that occurred on September 18, 2009 (M*w* 5.7) and May 31, 2010 (M*w* 5.9). We used three one-dimensional crust structure models to compute Green's functions. They were model iasp91 and the two other models (J1 and S1) from CRUST 2.0. The obtained solutions of the focal mechanisms were compared to the Global CMT. In terms of focal mechanisms and variance reductions, we obtained better solutions when we used model J1 as a crust structure. We performed inversions over a range of source depth. The variations of variance reductions as a function of depths show the clear peaks, which suggests that it is possible to determine a good focal depth. It is difficult to have a tight constraint for focal depth using the variance of residuals divided by the percent double-couple in our analyses. Since another seismic station in the study area has been upgraded to a broadband station recently, it will be possible to improve the accuracy of focal mechanism determination by the procedure used in this study.

Keywords: Focal mechanism, moment tensor, broadband waveform, velocity structure.

1. INTRODUCTION

Focal mechanisms provide important information for seismotectonic and hazard studies to regions such as the Philippines, where about twenty earthquakes occur everyday. Each earthquake radiates seismic waves that travel through the earth and are recorded by the seismic stations on the surface. Seismic waves are practically the only signal that can penetrate into the depth of the earth and bring back information about the interior of the earth.

Moment tensor/Focal mechanism analysis involves fitting theoretical waveforms with observed broadband waveforms to determine moment-tensor elements. A broadband seismic waveform carries the characteristics of earthquake source and structure along the propagation path. Given a set of seismograms and an appropriate structure model one can correct for propagation effects and obtain information on the source. Also, investigation using broadband waveform of local earthquakes can estimate seismic velocity structure (e.g., Dreger et al. 1990).

[*]Philippine Institute of Volcanology and Seismology–Department of Science and Technology, Philippines.
[**]International Institute of Seismology and Earthquake Engineering, Building Research Institute, Japan.

Since the broadband seismic stations in the country are continuously increasing in number, various seismological data analyses will be able to perform such as determination of focal mechanism solutions and an investigation of the crustal structure beneath these broadband recording stations. In the present study, we investigated the applicability of time domain moment tensor inversion by performing inversions using broadband data from an existing broadband station in the Philippines. We used three crust models to investigate which is more appropriate for the study region.

2. DATA

2.1 DAV Station

The station DAVAO (DAV) is located in the city of Davao on the island of Mindanao, southeastern Philippines. It is located in an area of intense seismicity and complex tectonics. Digital broadband seismic data from DAV station has been available since 1994 and can be accessed from the Incorporated Research Institutions for Seismology-Data Management Center (IRIS-DMC).

2.2 Event Selection

The focal depth is less than 40 km. The epicentral distance is less than 200 km. The short epicentral distances help to reduce possible errors introduced by the differences between the velocity model and the true ground structure such as scattering effects and phase shifts.

The seismograms used in this study are from two moderate crustal earthquakes. The 1st event is an M*w* 5.7 occurred on 18 September 2009, its origin time is 11:53:51.8 GMT (USGS). The 2nd event is an M*w* 5.9 recorded on 31 May 2010, its origin time of 10:16:03.4 GMT (USGS). Both earthquakes have clear seismic data recorded for the three components, which is an essential to determine the focal mechanism solution.

3. THEORY AND METHODOLOGY

3.1 Time Domain Moment Tensor Inversion

We used the time domain moment-tensors inversion code TDMT_INVc developed by Dreger (2003) to determine seismic moment tensors by inversion of three-component broadband waveform. The code is designed to obtain reliable solutions using a minimal number of stations based on the paper of Dreger and Helmberger (1993). In this study we used three component broadband seismogram from a single station.

3.1.1 Data Preparation

Preparation of the observed waveforms consists of the followings: 1) removing the instrument response, 2) rotation of the horizontal components to radial and transverse components, 3) integration to convert displacement, 4) passband filtering between 0.02 Hz and 0.05 Hz, 5) re-sampling the data to 1 sample per second to match the Green's functions. The Green's functions are filtered with the same passband filter for the observed data. Figure 1 shows the observed waveforms and the filtered seismograms.

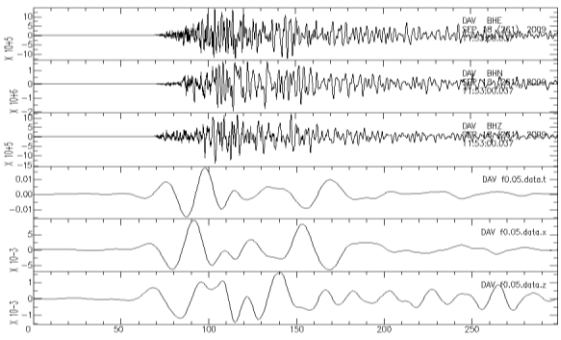

Figure 1. The observed waveform for the event 18 September 2009 (the upper three traces). The lower three traces are the time series obtained after the procedure explained in 3.1.1 is applied.

3.1.2 Computation of Green's Function

We generate a suite of Green's function over a range of source depth for each source-station distance using the available crustal models for the calculation of the Green's function to model the observed waveforms. The frequency-integration program (Saikia 1994) is used to compute the Green's functions to invert the synthetic waveform data. Subsequently, inverse Fast Fourier Transform (FFT) was performed to construct an eight-component waveform data in ASCII format. The ordering of the components is as follows: transverse component vertical strike slip (*tss*) and vertical dip slip (*tds*) faults, radial component vertical strike-slip (*xss*), vertical dip-slip (*xds*) and 45-degree dip-slip (*xdd*) faults, vertical component vertical strike slip (*zss*), vertical dip-slip (*zds*), and 45-degree dip slip (*zdd*) faults (Jost and Hermann 1989). An acausal (two pass) 4th order Butterworth filter is applied using Seismic Analysis Code (Goldstein et al., 2007) for the seismic waveform analyses. The frequency passband for both data and Green's function use the same filter. Figure 2 shows am example of the filtered functions for the eight components. The ordering of the components is described as the same manner as mentioned in the computation for Green's function. The same passband filter is applied to the Green's function.

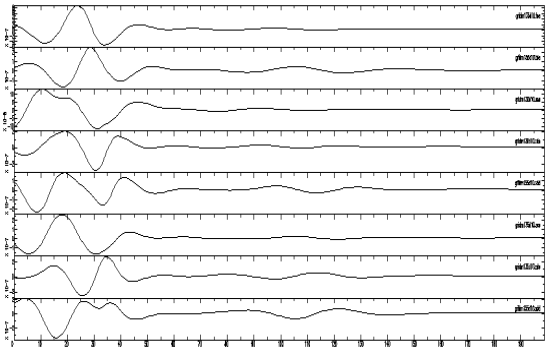

Figure 2. Green's functions for the eight components. (see text for details)

3.1.3 Moment Tensor Inversion

The observed seismograms are assumed to be represented by the following equation,

$$U_n(x,t) = M_{ij} \cdot G_{ni,j}(x,z,t) \tag{1}$$

where, U_n is the observed n^{th} component of displacement.
G_{nij} is the nth component Green's function for specific force couple orientations.
M_{ij} is the scalar seismic moment tensor.
i, j indices refer to the geographical directions.

M_{ij} describes the strength of the force-couples. The general force-couples for a deviatoric moment tensor are represented by vertical strike-slip, vertical dip-slip and 45 degree dip-slip. Linear least squares for deviatoric moment tensors are performed for Eq. (1).

To determine the source depth, inversions are performed over a range of source depths taking the best solution with the largest variance reduction (e.g., Dreger and Helmberger 1993) defined by:

$$VR = \left(1 - \frac{\sum_{i=0}^{N}(data_i - synth_N)^2}{\sum_{i=0}^{N}(data_N)^2}\right) \tag{2}$$

where, $data_i$ is the observed waveform.
$synth_N$ is the synthetic waveform.
VR is the variance reduction.
and the summation is performed for all components.

Another useful measurement for determining source depth is the RES/Pdc or variance of residuals divided by the percent double-couple defined by:

$$\frac{RES}{Pdc} = \frac{\sum_{i=0}^{N}(data_i - synth_N)^2}{Pdc} \tag{3}$$

where, *RES* is the residual variance and *Pdc* is the percent double-couple (the ratio of double couple component to total seismic moment). Dividing the variance by percent double–couple tends to deepen the minimum. The $data_i$ and $synth_N$ are the data and Green's function time series.

3.2 Construction of 1-D crust models

We constructed velocity models using CRUST2.0. This global crustal model uses a type key to assign crustal structure at a 2x2 degree model which composed of 360 key one-dimensional profiles, where one of these profiles is assigned to each 2x2 degree cell (Bassin et al. 2000).

Figure 3 shows the assigned crust types in our study region. The crustal velocity comprises of model J1 for an island arc, model S1 for the continental slope with a transition of 1 km sediments. In addition, model iasp91 model (Kennett et al. 1991) was also used in this study for earth structure comparisons. Figure 4 shows P-wave velocities of the three models. The water layer for model S1 was removed since the ray path travels mainly beneath the land area. This model was used as a possible model with a thinner crust.

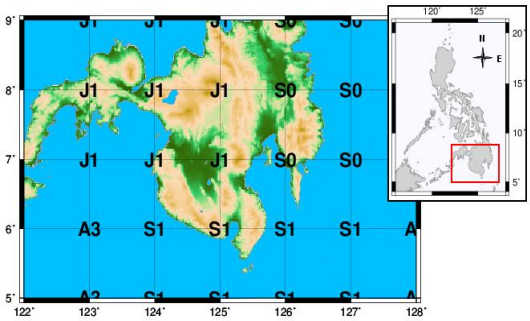

Figure 3. The key codes of CRUST2.0 for the study region. The upper right panel shows the location of the study region in the red rectangular.

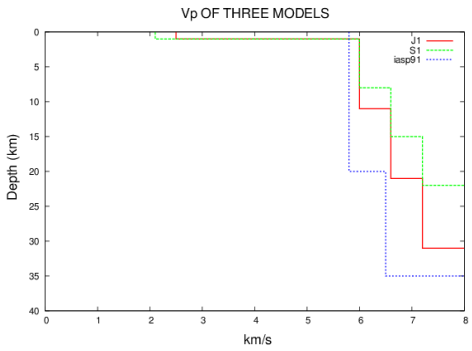

Figure 4. The red lines, dashed green lines and blue lines denote P-wave velocities of models J1, S1 and iasp91, respectively.

4. RESULTS AND DISCUSSION

4.1 Event 18 September 2009

Figure 5 shows the focal mechanism obtained for model J1 in case a depth is set to 5 km, which gives the largest variance reduction for this model. The comparison between the observed waveform denoted by the solid curves, and the synthetic waveform denoted by the dashed curves, is also shown in the same figure. The obtained focal mechanisms for model J1 at different depths are shown in Figure 6.

We applied a passband filter with corner frequencies between 0.02 Hz and 0.05 Hz to the observed seismograms. We found a better solution when this passband filter was used. In terms of variance reduction and focal mechanism, model J1 provides the better solution than the other two models. Figure 7 shows the variance reduction for model J1. For both models S1 and iasp91, the largest variance reductions are obtained for a depth of 5 km. Their focal mechanisms are shown in Figure 8 and Figure 9.

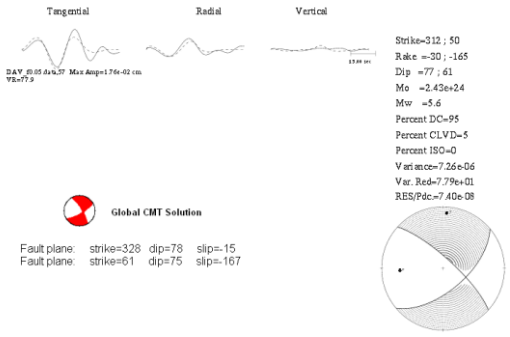

Figure 5. Moment tensor solution for model J1 with a depth of 5 km. The Global CMT solution is also shown.

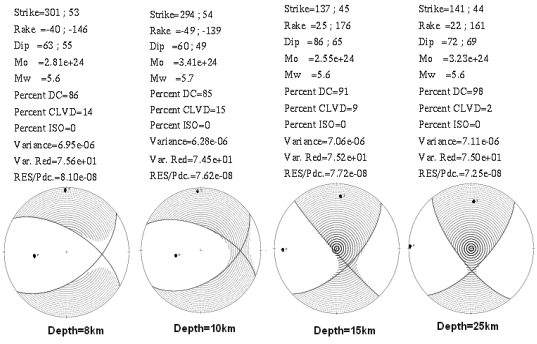

Figure 6. Variation of moment tensor solutions with different depths for model J1.

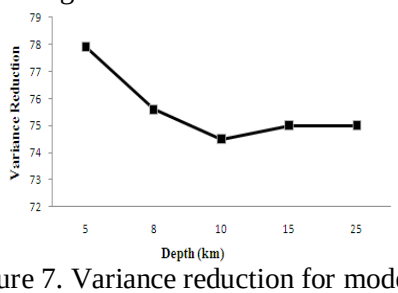

Figure 7. Variance reduction for model J1

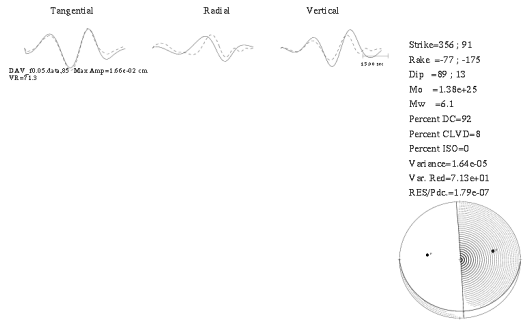

Figure 8. Moment tensor solution for model S1 with a depth of 5 km.

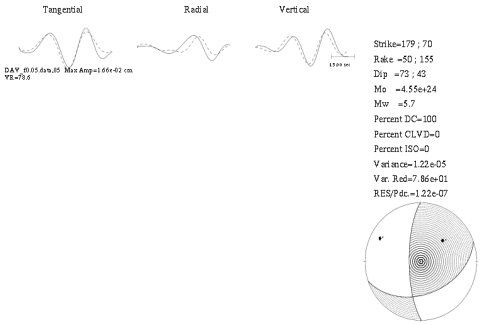

Figure 9. Moment tensor solution for model iasp91 with a depth of 5 km.

4.2 Event 2010 May 31

Figure 10 shows the focal mechanism obtained for the model J1 in case a depth is set to 9 km, which gives the largest variance reduction for this model. The comparison between the observed waveform denoted by the solid curves, and the synthetic waveform denoted by the dashed curves, is also shown in the same figure. The obtained focal mechanisms for model J1 at different depths are shown in Figure 11. The focal mechanism obtained for the model S1 at depth of 5km is shown in Figure 12. Figure 13 is the focal mechanism obtained for models iasp91 when depth is set to 23 km. Among the three crust models used, model J1 provides the better solution. Figure 14 shows change of variance reduction as a function of depth for the three crust models used.

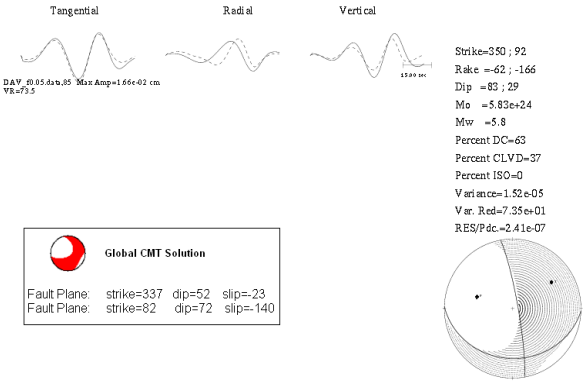

Figure 10. Moment tensor solution for the J1 model with depth of 9 km. The Global CMT solution is also shown.

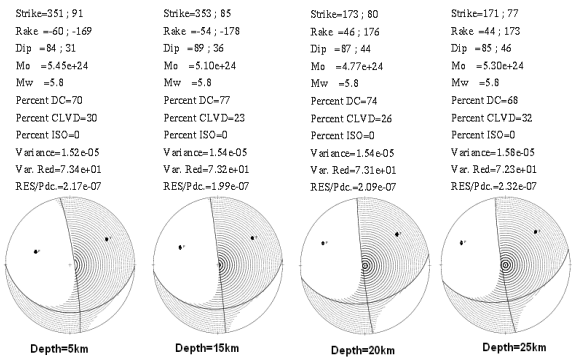

Figure 11. Variation of moment tensor solutions with different depths for model J1.

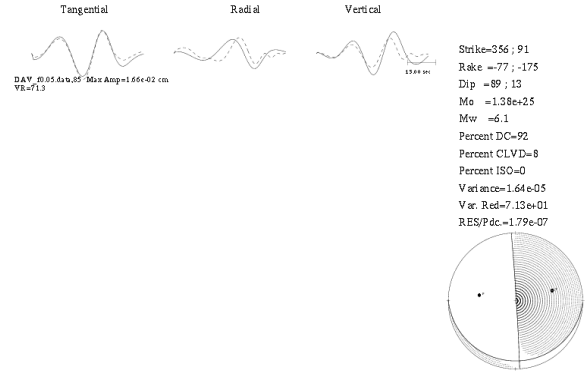

Figure 12. Moment tensor solution for model S1 with depth of 5 km.

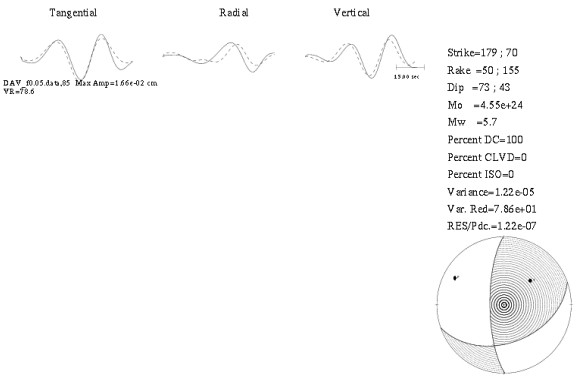

Figure 13. Moment tensor solution for model iasp91 with depth of 23 km.

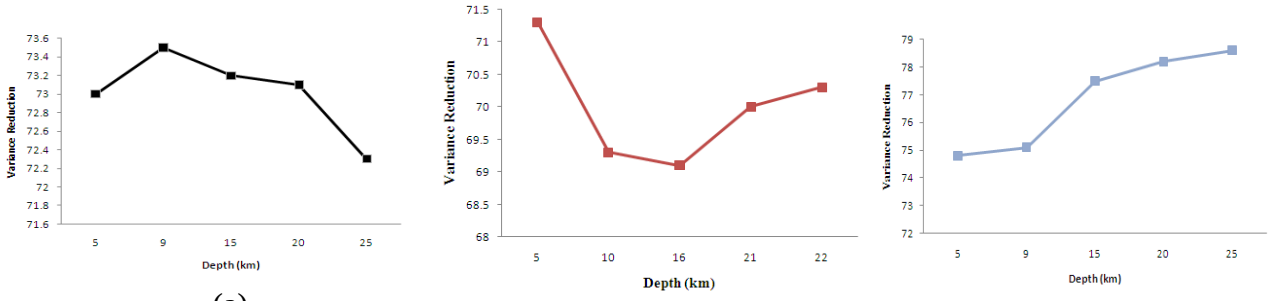

(a) (b) (c)

Figure 14. Change of variance reduction a function of depth for (a) model J1 (b) model S1 (c) model iasp91, respectively.

5. CONCLUSIONS

In this study, we performed time domain moment tensor inversion using a broadband waveform data recorded at one of the broadband seismic stations in the Philippines. We applied time domain moment tensor inversion code (TDMT_INVc) developed by Dreger (2003). We utilized broadband waveform data recorded at DAV seismic station. The seismograms were requested and retrieved from IRIS-DMC.

We analyzed two crustal earthquakes. They are the events on September 18, 2009, M*w* 5.7 and May 31, 2010 M*w* 5.9. Three one-dimensional crust structures were used for the calculation of Green's function to model observed waveform data. They are model iasp91and the two models (J1 and S1) from CRUST2.0. The results of our focal mechanism were compared to the Global CMT solution to investigate its reliability. Among the three crust structures used, model J1 provided the better solutions. We generated a suite of Green's function over a range of source depth. Our result shows that the variance reduction as functions of depths shows the clear peaks, which implies that it is possible to determine a good focal depth. On the other hand, the behavior of the variance of residuals divided by the percent double-couple seems complex.

Recently, another seismic station in the study area has been upgraded to a broadband station; data from this station will help to improve the accuracy of focal mechanism determination by the procedure used in this study.

ACKNOWLEDGEMENT

I would like express my sincere gratitude to Toshiaki Yokoi, Dr. Nobuo Hurukawa, Dr. Bartolome C. Bautista, Dr. Ma. Leonila P. Bautista, Mr. Ishmael Narag and Dr. Renato U. Solidum Jr for the support and valuable comments. We used Generic Mapping Tools (GMT) (Wessel and Smith 1998) for some of the figures in this study.

REFERENCES

Aki, K., and Richards, P.G., 1980, W. H. Freeman and Co., New York, San Francisco, 932 pp
Dreger, D. S., and D. V. Helmberger, 1990, Bull. Seism. Soc. Am., 80, 1162-1179.
Jost, M. L., and Hermann, R. B., 1989, Seism. Res. Lett., 60, 37-57.
Helmberger, D., Stead R., Ho-Liu P., and Dreger D., 1992, Geophys. J. Int. 110, 42-45.
Dreger, D. S., 2003, International Handbook of Earthquake and Engineering Seismology, B. 1627.
Dreger, D. S., and Helmberger, D. V., 1993, Geophys. Res., 98, 8107-8125.
Bassin, C., Laske, G., and Masters, G., 2000, EOS Trans AGU, 81, F897.
Kennett, B. L. N., and Engdahl, E. R., 1991, Geophys. J. Int., 105, 429-465
Goldstein, P., et al. http://www.iris.edu/manuals/sac/manual.html, 2007
Wessel, P. & Smith, W. H. F., 1998. Eos, Trans. Am. geophys. Un., 79, 579